Purification and Fluorescent Labeling of the Human Serotonin Transporter

Søren G. F. Rasmussen* and Ulrik Gether*

The Molecular Neuropharmacology Group, Department of Pharmacology, The Panum Institute, University of Copenhagen, DK-2200 Copenhagen, Denmark

Received September 14, 2004; Revised Manuscript Received December 21, 2004

ABSTRACT: To establish a purification procedure for the human serotonin transporter (hSERT) we expressed in Sf9 insect cells an epitope-tagged version of the transporter containing a FLAG epitope at the N-terminus and a polyhistidine tail at the C-terminus (FLAG-hSERT-12H). For purification, the transporter was solubilized in digitonin followed by nickel affinity and subsequent concanavalin A chromatography. Using this procedure we were able to obtain an overall purification of 700-fold and a yield of ∼0.1 mg/L of cell culture. The purified transporter displayed pharmacological properties similar to those of hSERT expressed in native tissues and in transfected cell lines. Fluorescent labeling of the purified transporter with the thiol-reactive fluorophore nitrobenxoxadiazol-iodoacetamide (IANBD) and Texas Red bromoacetamide preserved the pharmacological profile of FLAG-hSERT-12H. Collisional quenching experiments revealed that the aqueous quencher iodide was able to cause marked quenching of the fluorescence of the IANBD labeled transporter with a K_{SV} of 3.4 ± 0.10 M^{-1}. In a mutant transporter with five cysteines mutated (5CysKO) we observed a significant reduction in this quenching (K_{SV} = 2.1 ± 0.16 M^{-1}, $p < 0.01$). This reduction was most likely due to labeling of ^{109}Cys since mutation of this cysteine alone resulted in a reduction in collisional quenching that was similar to that observed with 5CysKO (K_{SV} = 2.2 ± 0.15 M^{-1}). These data suggest that labeling of ^{109}Cys contributes substantially to the overall fluorescence of IANBD labeled FLAG-hSERT-12H. On the basis of these data we infer that ^{109}Cys is embedded in a mixed hydrophobic/hydrophilic environment at the external ends of transmembrane segments 1 and 2. Further use of fluorescent techniques on purified hSERT should prove useful in future studies aimed at understanding the molecular structure and function of Na^+/Cl^--dependent neurotransmitter transporters.

Termination of monoaminergic neurotransmission is mediated via the action of three distinct, but highly homologous, transporters in the presynaptic membrane, the serotonin transporter (SERT), the dopamine transporter (DAT),[1] and the norepinephrine transporter (NET). These transporters serve as targets for many psychoactive compounds including both antidepressants and commonly abused drugs, such as cocaine and amphetamine. The SERT, DAT, and NET belong to the family of Na^+/Cl^--coupled transporters that also includes transporters for other neurotransmitters, such as glycine and γ-amino butyric acid (GABA).

Little is known about the tertiary structure of this class of transporters. Considerable evidence supports the presence of 12 putative transmembrane segments (TMs) connected by alternating extracellular and intracellular loops with an intracellular location of the N- and C-termini (Figure 1) (*1*, *2*). A high-resolution structure is, however, not yet available for any of these transporters, and our insight into the packing of the twelve helices remains limited (*1*, *2*). At present, the only available proximity relationships in the tertiary structure of this family of transporters are derived from identification and engineering of high-affinity Zn^{2+} binding sites in the DAT, SERT, GAT-1, and glycine transporter-1b (GlyT1b) (*3*−*8*). Interestingly, evidence suggests that Na^+/Cl^--coupled transporters exist in the membrane as oligomeric structures. The stoichiometry of the oligomeric complex is not yet clear, but recent studies using a cysteine cross-linking strategy indicated that the DAT forms a tetramer (*9*−*12*). It is noteworthy that the structures of two secondary active transporters, lactose permease and the glycerol-3-phosphate transporter (GlpT) from *Escherichia coli*, were recently solved at high resolution (*13*, *14*). The structures revealed the transporters in their putative inward facing conformation with the substrate binding site exposed to the intracellular milieu. However, neither of these two transporters displays any homology to the Na^+/Cl^--coupled transporters except for the presence of 12 transmembrane helices. Thus, to what degree the structure of lactose permease and GlpT mimics that of the Na^+/Cl^--coupled transporters remains an open but highly interesting question.

In addition to knowing little about the tertiary structure of Na^+/Cl^--coupled transporters, we have also limited insight

* Mailing address for correspondence: The Molecular Neuropharmacology Group, Department of Pharmacology 18-6, The Panum Institute, University of Copenhagen, DK-2200 Copenhagen N, Denmark. Tel: +45 3532 7548. Fax: +45 3532 7610. E-Mail: SGFR@neuropharm.ku.dk; gether@neuropharm.ku.dk.

[1] Abbreviations: hSERT, human serotonin transporter; DAT, dopamine transporter; NET, norepinephrine transporter; GAT1, γ-amino butyric acid (GABA) transporter-1; GLYT1b, glycine transporter-1b; GlpT, glycerol-3-phosphate transporter; CNX, calnexin; Con A, concanavalin A; IANBD, *N*,*N*′-dimethyl-*N*-(iodoacetyl)-*N*′-(7-nitrobenz-2-oxa-1,3-diazol-4yl)-ethylenediamide; TM, transmembrane; 5CysKO, FLAG-hSERT-12H containing mutations C15S, C21S, C109A, C522S, and C622A; 5-HT, 5-hydroxytryptamine; RTI-55, 3β-(4-iodophenyl)-tropane-2β-carboxylic acid methyl ester; MTSEA, ethanethiosulfonate ethylammonium; TEMPO, 2,2,6,6-tetramethylpiperidine-*N*-oxyl; PMSF, phenylmethylsulfonylfluoride; PP2A, protein phosphatase 2A; WT, wild-type.

10.1021/bi048022b CCC: $30.25
Published on Web 02/11/2005

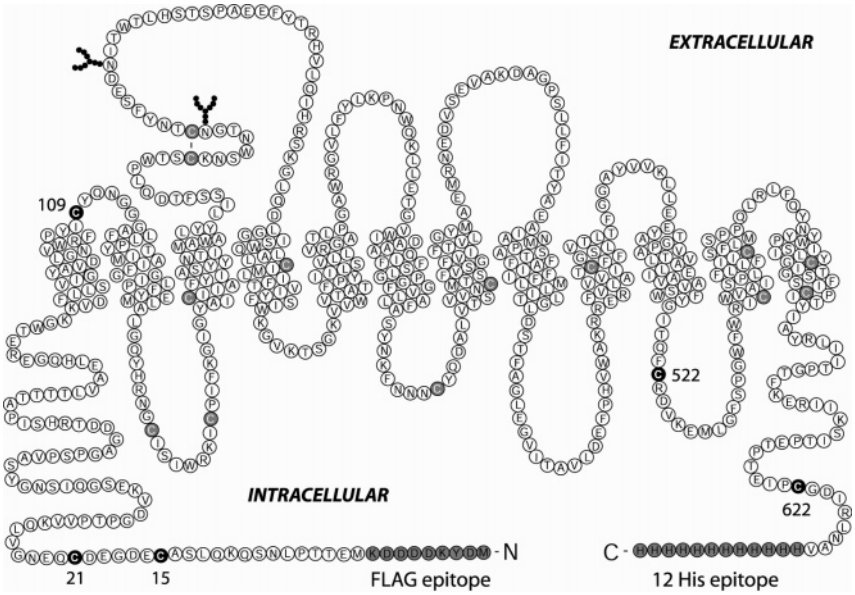

FIGURE 1: Snake representation of the epitope tagged hSERT. The hSERT contains 18 cysteines shown with white letters in gray or black circles. The cysteines knocked out in the hSERT-5CysKO construct are shown with white letters in black circles. The FLAG M2 immunodetection epitope and the 12 histidine epitope for nickel affinity chromatography (black letters in gray circles) were cloned on the amino- and carboxy-terminal tail, respectively. The N-linked glycosylation in extracellular loop 2 was utilized for the Con A affinity chromatography.

into the predicted large-scale conformational changes responsible for the substrate translocation process. Several biochemical and electrophysiological approaches have been applied and provided some information about conformationally active domains (*1*, *2*, *15*), but still the character and dynamics of the conformational changes remain poorly understood. This might at least in part be due to the fact that e.g. fluorescence techniques on purified transporter preparations, which have proven very useful for studying the molecular function of other membrane proteins, have not yet been applied to this family of proteins. Notably, the application of fluorescent technique to the β2 adrenergic receptors (*16*−*19*) and the Lac permease of *Escherichia coli* (*20*, *21*) has provided substantial insight into the molecular function of these proteins.

In this study we have sought to establish a system that allows for fluorescent as well as for other biophysical analyses of a Na^+/Cl^--coupled transporter. To achieve this goal we expressed an epitope-tagged version of the human SERT in Sf9 insect cells and established a purification procedure using a combination of nickel chromatography and concanavalin A chromatography. We show here that in this way we have been able to obtain sufficient and sufficiently pure transport protein for spectroscopic studies. We also show that the purified transport protein has pharmacological properties similar to those of the transporter in native tissue and that it can be derivatized with specific fluorophores without perturbing its ligand binding properties. Moreover, we provide evidence that a cysteine situated in the short extracellular loop between TM1 and 2 is a labeling site for the environmentally sensitive fluorophore IANBD. The data suggest that the cysteine is situated in a mixed hydrophobic environment consistent with its localization close to the predicted but not yet experimentally verified membrane/surface border. Altogether, the current data support the prospect of applying spectroscopic techniques to unravel the molecular function of Na^+/Cl^--coupled transporters in further detail.

EXPERIMENTAL PROCEDURES

Mutagenesis. Using the Pfu polymerase (Stratagene, La Jolla, LA) for the PCR and primers containing the FLAG epitope with an upstream *Not*I restriction site and primers encoding a 12-histidine tag with a downstream *Xba*I restriction site, the hSERT was tagged at the amino- and carboxy-terminus, respectively resulting in FLAG-hSERT-12His. The cDNA encoding FLAG-hSERT-12His tagged transporter was inserted into the mammalian expression vector pUbi1z (*22*). To facilitate the mutagenesis the cDNA encoding hSERT was modified with a silent *Pvu*I site in position 724, a *Mfe*I site in position 1684, and a *Hin*dIII site in position 955 silently knocking out a *Mfe*I site. The additional restriction sites and the cysteine knock-out mutants of the hSERT cDNA were generated by PCR-derived mutagenesis using Pfu polymerase according to manufacturer's instructions (Stratagene). The generated PCR fragments were cleaved with the appropriate restriction enzymes, purified by agarose gel electrophoresis, and cloned into the pUbi1z FLAG-hSERT-12His construct. Subsequently, the transporter constructs were cloned into the Sf9 insect cell vector pVL1392 (BD Biosciences Pharmingen, San Diego, CA) via the *Not*I and *Xba*I sites. Mutations were confirmed by restriction enzyme analysis and DNA sequencing using an automated ABI 310 sequencer (Applied Biosystems, Foster City, CA) according to manufacturer's instructions.

Expression in Sf9 Insect Cells. Sf9 insect cells were maintained in SF-900 II medium supplemented with 5% heat inactivated fetal calf serum (Invitrogen) and 0.01 mg/mL gentamicin at 27 °C either as monolayer cultures in tissue culture flasks or as suspension cultures in Erlenmeyer flasks under constant rotation (120 rpm). For expression in Sf9 insect cells hSERT, hSERT-5CysKO (containing the cysteine knock-out mutations C15S, C21S, C109A, C522S, C622A), and hSERT-C109A in the pVL1392 vector were co-infected with linerized baculovirus DNA (BD Biosciences Pharmin-

gen) into Sf9 insect cells according to the manufacturer's instruction (BD Biosciences Pharmingen). Baculovirus containing the canine molecular chaperone calnexin (CNX) was kindly provided by Dr. Chris Tate, MRC Cambridge, U.K. Baculovirus encoding the transporter constructs and CNX were isolated by plaque purification and through several rounds of amplification high titer virus stocks were obtained ($\sim 10^9$ plaque forming units/mL).

Purification Procedure. For purification, insect cells were grown in 1 L cultures at a density of 2 million cells/mL. The culture was co-infected with 1:25 of a high titer virus stock of the hSERT and 1:12 dilution CNX. The cells were harvested 48−64 h later by centrifugation (10 min at 5000*g*) and the pellet kept at −80 °C until purification. The transporter was purified using a two-step purification procedure. One pellet of Sf9 cells from 1 L of infected culture was resuspended in ice-cold lysis buffer (25 mM Hepes pH 7.4 with 10 μg/mL leupeptin, 10 μg/mL benzamidine, and 1 mM phenylmethylsulfonylfluoride (PMSF)). Following centrifugation (30000*g* for 30 min at 4° C) the lysed cells were resuspended in buffer (25 mM Hepes pH 7.4, 30% glycerol, 100 mM NaCl, 10 μg/mL leupeptin, 10 μg/mL benzamidine, and 1 mM PMSF) containing 1% digitonin (Calbiochem, San Diego, CA) and homogenized in a Dounce homogenizer (25 strokes with the tight pestle) and stirred for 2 h at 4 °C. Following centrifugation (30000*g* for 30 min at 4 ° C) the solubilized transporter was incubated under rotation with 18 mL of nickel equilibrated chelating sepharose (Amersham Biosciences, Piscataway, NJ) for 2 h at 4 °C containing 2 mM imidazole and 300 mM NaCl. The nickel column was washed with 8 columns of ice cold wash buffer (25 mM Hepes pH 7.4, 0.1% digitonin, 10% glycerol, 300 mM NaCl) containing 2, 5, 10, 20, 30, 40, 50, and 60 mM imidazole, respectively. [^{125}I]RTI-55 binding activity was eluted in 500 μL fractions using wash buffer containing 200 mM imidazole. Fractions containing SERT were pooled and further purified using concanavalin A (Con A) resin (Amersham Biosciences). The nickel pure SERT was incubated for 2 h at 4 °C with 1000 μL of Con A agarose equilibrated in wash buffer. The resin was washed with 15 columns of ice cold buffer. Elution was performed by stopping the column flow and adding wash buffer containing 250 mM α-methyl-mannopyranoside. The resin was resuspended in the elution buffer several times during the 45 min incubation time at room temperature. Two to three consecutive batch elutions were performed. The eluted Con A pure protein was concentrated using Centricon YM-30 spin concentrators (Millipore, Billerica, MA).

Labeling with Fluorescent Probes. For fluorescence spectroscopy the transporter constructs were labeled with the fluorescent probes on the Con A resin. Usually about 1−2 nmol of hSERT eluted from the nickel affinity sepharose was incubated with 500 to 1000 μL of Con A resin in a 15 mL tube on slow rotation for 90 min at 4 °C. Then 100 μM *N*,*N*′-dimethyl-*N*-(iodoacetyl)-*N*′-(7-nitrobenz-2-oxa-1,3-diazol-4-yl)ethylenediamine (IANBD) (Molecular Probes, Eugene, OR) or 200 μM Texas Red C_5 bromoacetamide (Molecular Probes) was added and the incubation continued in darkness for another 30 or 45 min, respectively. The reaction was quenched by addition of 1 mM cysteine. The Con A resin was transferred to a Poly Prep column (Bio-Rad, Hercules, CA) and washed extensively (30−40 column volumes) in ice cold wash buffer (25 mM Hepes pH 7.4, 0.1% digitonin, 10% glycerol, 300 mM NaCl) and eluted in wash buffer containing 250 mM α-methyl-mannopyranoside and spin concentrated as described above. For the initial fluorescence labeling experiments, hSERT expressed in Sf9 cell membranes was labeled for 30 min at 4 °C under slow rotation in the presence of 500 μM IANBD or Texas Red. For the MTSEA experiments Sf9 cell membranes were incubated for an additional 15 min period in the presence or absence of 2 mM MTSEA at RT. Purified hSERT was labeled in the presence of 100 μM IANBD or 200 μM Texas Red in vials under slow rotation at 4 °C for 30 and 45 min, respectively. As control, unlabeled hSERT received analogous treatment. The B_{MAX} values of the control and labeled hSERT were estimated from homologous competition binding using 0.25 nM [^{125}I]RTI-55 as radioligand according to methods described below.

Ligand Binding Assays. Binding experiments on hSERT expressed in Sf9 insect cell membranes and of the purified transporter were performed using [^{125}I]RTI-55 (NEN, Boston, MA) as radioligand. In competition binding assays on membranes, 5 μg of membrane protein was assayed in a total volume of 250 μL using a sodium phosphate buffer (50 mM Na_2HPO_4/NaH_2PO_4, pH 7.4) containing 0.25 nM [^{125}I]RTI-55 and increasing concentrations of competing ligands, 5-HT, citalopram, imipramine, cocaine, or RTI-55. The membranes were incubated for 2 h at room temperature before separation of bound from unbound by rapid filtration over glass fiber filters (FilterMat B) (Wallac, Turku, Finland) using a Tomtec 96-well cell harvester. MeltiLex Melt-on scintillator sheets (Wallac) were used for counting of the filter in a Wallac Tri-Lux β scintillation counter. Competition binding experiments on purified transporter (15 fmol of transporter) were performed in digitonin buffer (25 mM Hepes pH 7.4, 0.1% digitonin, and 150 mM NaCl) in a total volume of 100 μL using 0.25 nM of [^{125}I]RTI-55 and increasing concentrations of unlabeled ligands. The binding assays were incubated at room temperature for 30 min before separation of bound from unbound on 2 mL Sephadex G-50 columns (Amersham Biosciences). The eluate was collected directly in 4 mL counting vials (Wallac) using 1000 μL of ice-cold digitonin buffer. HiSafe scintillation fluid (Wallac) was added, and the vials were counted in a Wallac Tri-Lux β scintillation counter. To estimate the B_{MAX} of hSERT in pellets, membranes, and of the purified transporter, [^{125}I]RTI-55 binding was performed using a single subsaturating concentration of the radioligand (0.5 nM) in the presence and absense of 10^{-5} M RTI-55. B_{MAX} was calculated by the equation $B_{MAX} = B_0(1 + K_d/[\text{radioligand}])$. Binding was assayed using the same buffers and method of separation as described above. All determintaions in the binding assays were done in triplicate. Binding data were analyzed by nonlinear regression analysis using Prism 2.0 from GraphPad Software, San Diego, CA.

Fluorescence Spectroscopy. Fluorescence spectroscopy was performed on a SPEX Fluoromax-2 spectrofluorometer connected to a PC equipped with the Datamax 2.2 software package (Jobin Yvon Inc., Edison, NJ). In all experiments the excitation and emission band-pass were set at 5 nm. The excitation and emission scans were performed on 10 pmol of IANBD or Texas Red labeled transporter added to a 5 × 5-mm quartz cuvette (Helma, Mulheim, Germany) containing

400 μL of buffer (25 mM Hepes, 150 mM NaCl, 0.1% digitonin, pH 7.4). Excitation scanning of the IANBD labeled hSERT between 400 and 528 nm was obtained by recording emission at 540 nm. IANBD emission scanning was measured from 495 to 625 nm with excitation set at 480 nm. Excitation scanning of the Texas Red labeled hSERT between 400 and 630 nm was obtained by recording emission at 640 nm. For Texas Red emission scanning, excitation was set at 550 nm and emission was recorded from 560 to 675 nm. Emission scans of IANBD free in water or dioxane/water mixtures were measured from 495 to 625 nm with excitation set at 480 nm. The excitation and emission spectra are averages of three consecutive scans obtained with an integration time of 0.3 s/nm. The spectra were corrected for any background fluorescence by routinely subtracting control spectra on buffer alone.

Fluorescence Anisotropy. The SPEX Fluoromax-2 spectrofluorometer was equipped with an automated L-format polarization accessory including two Glan-Thomson UV polarizers placed in the sample chamber to enable polarized excitation and emission detection. The anisotropy measurements were carried out using the Constant Wavelength Analysis program with the excitation set at 480 nm and emission measured at 528 nm with a 10 s integration time. Concurrent measurements of the emission intensity with the excitation-side polarizer in the vertical position (V) and the emission-side polarizer in either the V or horizontal position (H) were carried out. Measurements of fluorescence anisotropy on IANDB free in water or buffer (25 mM Hepes, 150 mM NaCl, 0.1% digitonin, pH 7.4), IANBD labeled to nickel affinity purified protein, and on the Con A purified and IANBD labeled hSERT was carried out at 20 °C. The data were converted to anisotropy according to the equation $A = (I_{VV} - GI_{VH})/(I_{VV} + 2GI_{VH})$, where I_{VV} is the intensity measured with both the excitation-side and emission-side polarizer in the vertical position (V), I_{VH} is the intensity measured with the excitation-side polarizer in the vertical position (V) and the emission-side polarizer in the horizontal position (H), and G is the ratio of the sensitivities of the detection system for vertically and horizontally polarized light (S_V/S_H) (*23*).

Fluorescence Quenching Experiments. Quenching experiments were performed on 10−20 pmol of IANBD labeled transporter in 400 μL of buffer. Stock solutions (1.0 M) of the hydrophilic quencher potassium iodide (KI) containing 10 mM $Na_2S_2O_3$ was prepared freshly for each round of experiments. The hydrophobic quencher TEMPO (2,2,6,6-tetramethylpiperidine-*N*-oxyl) was dissolved in 10% DMSO at a concentration of 100 mM and immediately used. To correct for dilution/ionic strength effects on fluorescence, measurements were performed in parallel using a 1.0 M stock of potassium chloride (KCl) and a 10% DMSO stock for the KI and TEMPO quenching experiments, respectively. Ten microliters of quencher (potassium iodide or TEMPO) or control solution (potassium chloride or 10% DMSO) was added sequentially followed by thorough mixing after each addition and subsequent recording of fluorescence using the Constant Wavelength Analysis program in the Datamax software package. The excitation wavelength was 480 nm, and the emission wavelength was 528 nm. In the experiments with TEMPO, the fluorescence intensities were corrected as described (*24*) for inner filter effects caused by the absorption by TEMPO at the used excitation and emission wavelengths. The corrected data were plotted according to the Stern−Volmer equation, $F_0/F = 1 + K_{sv}[Q]$, where F_0/F is the ratio of fluorescence intensity in the absence and presence of quencher (Q) and K_{sv} is the Stern−Volmer quenching constant (*23*).

Table 1: Purification of hSERT from Sf9 Insect Cells[a]

	yield ± SE (nmol)	purity ± SE (pmol/mg protein)	fold purification	
			stepwise	overall
Sf9 cell culture	15.2 ± 0.8	7.5 ± 1.1		
solubilized membranes	9.2 ± 1.3	26.9 ± 3.0	3.6	3.6
Ni^{2+} affinity pure	3.0 ± 0.2	1099 ± 395	41	148
Con A affinity pure	0.95 ± 0.2	5167 ± 1225	4.7	694

[a] The table shows the yield, purity, and fold purification at various stages of the purification procedure of FLAG-hSERT-12His. We used [^{125}I]RTI-55 binding activity to determine the amount of functional hSERT as described in the Experimental Procedures.

RESULTS

Expression and Purification of the hSERT. The cDNA encoding the human SERT was tagged at the C-terminus with 12 histidines and at the N-terminus with a FLAG epitope for expression in *Spodoptera frugiperda* (Sf9) cells (Figure 1). The expression level of the resulting construct (FLAG-hSERT-12His) was 8.0 ± 0.6 nmol of hSERT/1 L of culture (containing 2×10^9 Sf9 cells) as determined by [^{125}I]RTI-55 binding ($n = 4$). To increase the fraction of mature and correctly folded SERT (*25*), the insect cells were co-infected with baculovirus encoding the molecular chaperone calnexin (CNX). Coexpression with CNX increased the B_{MAX} to 14.5 ± 0.6 nmol of hSERT/culture ($n = 8$).

For purification, isolated insect cell membranes from one 1 L culture were solubilized in buffer containing 1% digitonin. The transporter was purified in two steps by nickel affinity and concanavalin A (Con A) chromatography. The nickel chromatography provided 41-fold purification whereas the subsequent Con A step added an extra 4.7-fold of purification (Table 1). Overall, we achieved 694-fold purification relative to the starting material, i.e., the cell lysate. The final purity of the hSERT following the Con A chromatography was 5.2 nmol/mg protein (Table 1) corresponding to 36% functional transporter as measured by [^{125}I]-RTI-55 binding. The purified hSERT analyzed by SDS-polyacrylamide gel electrophoresis and silver staining comprised 46% ± 8 (mean ± SE, $n = 6$) of the total protein (Figure 2). Hence, around 80% of the purified transporter is functional. In general about 1 nmol of hSERT (0.07 mg) could be obtained from 1 L of cell culture (Table 1).

Since a major goal of this study was to site-selectively label the hSERT with sulfhydryl-reactive probes, we wished to reduce the number of reactive cysteines in the transporter. We decided first to remove cysteines present outside the transmembrane region because we predicted that these could more likely be mutated without perturbing expression and/or function in comparison to transmembrane cysteines. With a minor change in expression (10.0 ± 1.9 nmol of hSERT/culture [$n = 6$]) we were able to remove five cysteines present outside the transmembrane region including C15S, C21S, C109A, C522S, and C622A resulting in hSERT-5CysKO. Mutation of additional residues outside the trans-

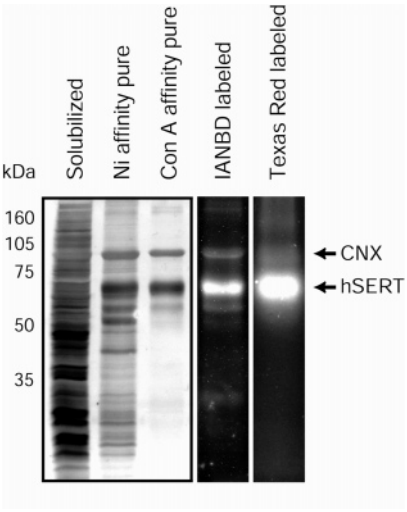

FIGURE 2: Purification and fluorescence labeling of hSERT. Samples at various stages of purification were separated on 10% SDS/polyacrylamide gel and silver stained (left panel) or imaged for fluorescence (the two right side panels). From left to right shows a sample of solubilized proteins from Sf9 cell membranes, a sample of the protein eluted from the nickel column, and a sample of protein eluted from the Con A resin. The solubilized protein in the SDS/polyacrylamide gel contains 20-fold less [^{125}I]RTI-55 binding activity than that loaded of the nickel and Con A pure protein. The fluorophore labeled hSERT was imaged in a Bio-Rad FluorS Imager using transluminant UV light for excitation of the IANBD or Texas Red fluorophores. Emission was recorded using the 520 nm long pass filter settings.

membrane region such as ^{147}Cys, ^{155}Cys, and ^{357}Cys decreased expression of this construct in Sf9 cells so profoundly that purification was essentially impossible (data not shown). Furthermore, additional mutation of transmembrane cysteines in hSERT-5CysKO, such as ^{166}Cys, ^{258}Cys, and ^{369}Cys, also had a dramatic negative impact on expression (data not shown). Thus, we decided to continue with hSERT-5CysKO in our labeling studies. In addition to hSERT-5CysKO we also studied a mutant in which ^{109}Cys was mutated to Ala (hSERT-C109A). The expression level of hSERT-C109A coexpressed with CNX was 8.0 ± 0.33 nmol of hSERT/culture (n = 7). Application of the purification protocol described above for the wild-type to C109A and 5CysKO resulted in the same purification efficiencies (data now shown).

The Purified SERT Retains Native Ligand Binding Properties. The pharmacological profile of the hSERT construct expressed in Sf9 cell membranes was assessed in competition binding experiments using [^{125}I]RTI-55 as radioligand (Table 2). The observed binding affinities were altogether within the same range as those observed previously in native transporter preparation derived from brain tissue and blood platelets (*26*−*28*) and in transfected mammalian cell lines (*29*−*34*). This supports proper folding of the epitope tagged transporter in the Sf9 cell membranes.

Subsequent competition binding on the Ni^{2+}/Con A affinity chromatography purified hSERT (Table 2) and hSERT mutants 5CysKO and C109A (Table 3) revealed substrate and inhibitor affinities that in general were similar to those obtained for the transporter in the Sf9 cell membranes (Table 2). For 5-HT we observed an apparent affinity in the purified preparation of ∼0.8 μM as compared to ∼8.3 μM in the Sf9 cell membranes. For citalopram and imipramine we observed 3- to 9-fold higher affinities whereas the affinities for cocaine and the cocaine analogue RTI-55 were essentially identical in membranes and in the purified transporter preparation (Table 2). Taken together, the results support the inference that the overall conformation of the transporters is conserved upon purification.

Fluorescent Labeling of hSERT Is Well Tolerated. To examine the sensitivity of hSERT toward cysteine-reactive fluorescent probes the transporter expressed in Sf9 membranes and upon purification was labeled with NBD iodoacetamide (IANBD) or Texas Red bromoacetamide. In the Sf9 cell membranes, labeling with either fluorophore resulted in a small increase in the K_i value for [^{125}I]RTI-55 (about 2-fold) without a significant change in the B_{MAX} (Table 4). A similar observation was done when reacting with the charged sulfhydryl-reactive reagent MTSEA (methanethiosulfonate ethylammonium) (Table 4). It is important to note that this does not disagree with previous reports showing marked inhibition of [^{125}I]RTI-55 binding to SERT in response to MTSEA (*35*). These assays were performed with a subsaturating concentration of the radioligand and under these conditions even a minor 2-fold decrease in affinity can cause a large decrease in apparent binding (B_0). This is directly illustrated by the binding curves in Figure 3 showing 40−50% reduction in B_0 for IANBD and MTSEA labeled transporter as the result of a 2-fold decrease in affinity with no change in B_{MAX} (Table 4). Interestingly, in both 5CysKO and C109A we did not see any change in [^{125}I]RTI-55 affinity upon IANBD labeling whereas a small decrease in affinity was still apparent in response to MTSEA (data not shown).

For the purified transporter we observed a similar scenario. In the hSERT wild type, labeling with IANBD or Texas Red bromoacetamide did not change B_{MAX} but caused a marginal decrease (1.5-fold) in affinity for [^{125}I]RTI-55 (Table 4). However, similar to our observations in membranes we did not see any affinity change for [^{125}I]RTI-55 in both 5CysKO and C109A (Table 3). This suggests that labeling of ^{109}Cys is responsible for the [^{125}I]RTI-55 affinity change seen in the wild-type hSERT in response to IANBD or Texas Red bromoacetamide. Of interest, labeling of ^{109}Cys appeared to have no impact on the affinities for cocaine, citalopram, imipramine, and 5-HT (Table 2). In fact, the affinity increased slightly for 5-HT (Table 2). Altogether, it seems reasonable, therefore, to conclude that the overall conformation of the transporters is conserved both upon purification and upon fluorescent labeling.

The covalent fluorescent labeling of the purified transporter was directly visualized by SDS−polyacrylamide gel electrophoresis followed by fluorescence imaging as illustrated in Figure 2. The two major bands corresponding to hSERT and CNX constituted 87% and 13% of the total transporter/CNX fluorescence, respectively as assessed by densitometry analysis (Figure 2). Similarly the Texas Red fluorescence from hSERT constituted 84% of the combined total transporter/CNX fluorescence. The combined fluorescence from transporter and CNX amounted ∼60% of the total fluorescence leaving ∼40% to background fluorescence from other protein impurities and aggregated hSERT running as high MW complexes. The high MW aggregate constitutes around 7% for both fluorescently labeled transporters.

Decreased Rotational Freedom of IANBD Labeled to the hSERT. Anisotropy represents a measure of molecular

Table 2: Binding Properties of Purified and Fluorophore Labeled hSERT in Comparison to hSERT in Sf9 Membranes[a]

	K_i [SE interval] (nM)			
	Sf9 membrane hSERT	purified hSERT	purified and IANBD labeled hSERT	purified and Texas Red labeled hSERT
5-HT	8270 [7360−9290]	823 [727−933]	303 [269−342]	284 [233−246]
RTI-55	0.60 [0.53−0.68]	0.60 [0.54−0.67]	0.92 [0.84−1.0]	0.85 [0.72−1.0]
cocaine	204 [189−220]	191 [168−217]	191 [166−220]	157 [133−185]
citalopram	8.7 [8.0−9.6]	3.0 [2.8−3.2]	4.0 [3.7−4.4]	3.3 [3.1−3.5]
imipramine	13.5 [12.0−15.1]	1.5 [1.3−1.6]	1.5 [1.4−1.7]	

[a] Competition binding on hSERT expressed in Sf9 insect cell membranes and on purified and fluorescently labeled transporter using 0.25 nM [^{125}I]RTI-55 as radioligand. The K_d values were calculated by the equation $K_d = IC_{50} -$ [radioligand]. The IC_{50} values used for calculation of K_i values were obtained from means of $pIC_{50} \pm$ SE. K_i values were calculated according to the equation $K_i = IC_{50}/(1 + L/K_d)$ where L is concentration of radioligand.

Table 3: Binding Properties of Purified and Fluorophore Labeled Cysteine Knock-Out Mutants of hSERT[a]

	K_i [SE interval] (nM)			
	purified hSERT 5CysKO	purified and IANBD hSERT 5CysKO	purified hSERT C109A	purified and IANBD labeled hSERT C109A
5-HT	296 [242−362]	362 [272−480]	556 [447−691]	575 [513−645]
RTI-55	0.71 [0.61−0.82]	0.89 [0.76−1.05]	1.24 [1.12−1.36]	1.0 [0.83−1.24]
cocaine	187 [157−221]	245 [227−264]	261 [211−324]	227 [199−259]
citalopram	4.3 [4.0−4.6]	4.4 [4.0−5−0]	4.7 [3.6−6.2]	4.1 [3.6−4.6]
imipramine	5.8 [5.1−6.5]	5.7 [5.1−6.5]	2.4 [1.9−3.1]	3.2 [2.9−3.7]

[a] Competition binding on purified and fluorescently labeled transporter mutants using 0.25 nM [^{125}I]RTI-55 as radioligand. The K_d values were calculated by the equation $K_d = IC_{50} -$ [radioligand]. The IC_{50} values used for calculation of K_i values were obtained from means of $pIC_{50} \pm$ SE. K_i values were calculated according to the equation $K_i = IC_{50}/(1 + L/K_d)$ where L is concentration of radioligand.

Table 4: Effect of Fluorescent Labeling on B_{MAX} of hSERT[a]

	$B_{MAX} \pm$ SE (% of unlabeled)	K_i [SE interval] (nM)
Sf9 membranes		
unlabeled SERT	100	0.60 [0.53−0.68]
IANBD labeled SERT	99.2 ± 7.3	1.3 [1.18−1.52]
Texas Red labeled SERT	82.4 ± 14.8	1.3 [1.13−1.49]
MTSEA labeled SERT	115.3 ± 25.2	1.4 [1.15−1.70]
purified		
unlabeled SERT	100	0.60 [0.54−0.67]
IANBD labeled SERT	98.0 ± 5.0	0.92 [0.84−1.01]
Texas Red labeled SERT	96.7 ± 3.8	0.85 [0.72−1.00]

[a] The hSERT was expressed in Sf9 cell membranes and labeled upon purification with IANBD and Texas Red as described in the Experimental Procedures. Briefly, the membranes were labeled in the presence of 500 μM IANBD or Texas Red and the purified transporter in the presence of 100 μM IANBD or 200 μM Texas Red. B_{MAX} values of control and labeled hSERT were estimated from homologous competition binding using 0.25 nM [^{125}I]RTI-55 as radioligand.

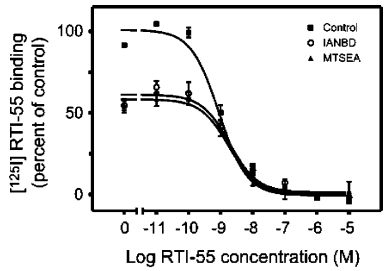

FIGURE 3: Effect of IANBD and MTSEA on hSERT. Sf9 membranes expressing hSERT were incubated in the absence (squares and triangles) or presence (open circles) of 500 μM IANBD for 30 min at 4 °C followed by treatment in the presence (triangles) or absence (squares and open circles) of 2 mM MTSEA for 15 min at RT. The effects of the treatments were measured by homologous competition binding using 0.25 nM [^{125}I]RTI-55 as radioligand. The binding affinity of RTI-55 to the control (squares), the membranes treated with IANBD (open circles), and MTSEA (triangles) was calculated using the equation $K_i = IC_{50}/(1 + L/K_d)$ to be 0.6, 1.3, and 1.4 nM, respectively. B_{MAX} is estimated from the equation $B_{MAX} = B_0(1 + K_d/[\text{radioligand}])$.

motions at a nanosecond time scale (*23*). Accordingly, steady-state anisotropy measurements were carried out to investigate the rotational freedom of free IANBD and IANBD labeled to the purified hSERT. The anisotropy of IANBD free in water was 0.049 ± 0.001 (means ± SE, n = 3) at 20 °C (data not shown) consistent with substantial rotational freedom. The anisotropy of IANBD free in buffer containing digitonin micelles was 0.126 ± 0.002 (means ± SE, n = 3) at 20 °C (Figure 4). This increase in anisotropy most likely reflects some degree of association of IANBD to the detergent micelles restraining the rotational freedom of the fluorophore. Following nickel affinity chromatography the eluted protein was labeled for 30 min at 4 °C in the presence of 100 μM IANBD. The anisotropy of this mixture was measured to a slightly larger value than the free IANBD revealing a residual excess of free IANBD compared to labeled protein, 0.146 ± 0.003 (means ± SE, n = 3) at 20 °C (Figure 4). After removing the remaining free IANBD by extensive washing on the Con A resin the labeled hSERT was eluted. The anisotropy of the purified and IANBD labeled hSERT was 0.322 ± 0.002 (means ± SE, n = 3) at 20 °C (Figure 4), indicating a significantly constrained rotational freedom of the fluorophores on the purified transporter. Interestingly, the same degree of anisotropy was achieved in the purified rat SERT upon binding of a fluorescent cocaine analogue RTI-233, containing an equivalent NBD fluorophore (*36*).

Evidence for IANBD Labeling Sites in Highly Hydrophobic Transporter Domains. The emission from IANBD is, in contrast to the Texas Red fluorophore, highly sensitive to the polarity of the environment. In water, we observed that the λ_{MAX} (wavelength at which maximum emission occurs) of IANBD was 542 nm when the optimal excitation

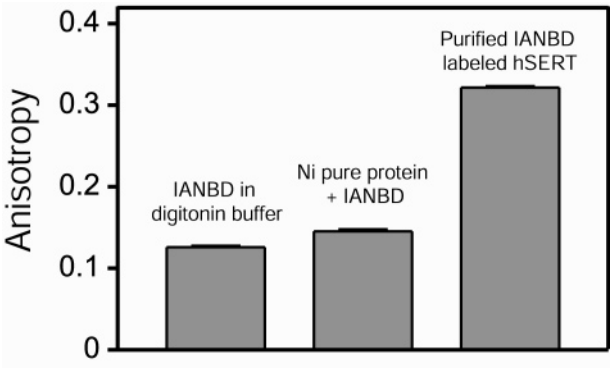

FIGURE 4: Fluorescence anisotropy of the purified and IANBD labeled hSERT in comparison to free IANBD and unwashed IANBD labeled nickel pure protein. Fluorescence anisotropy of IANBD free in digitonin buffer (left bar), of a diluted sample of a mixture containing nickel pure protein labeled for 30 min in the presence of 100 μM IANBD (middle bar), and of the IANBD labeled and Con A purified transporter in which excess IANBD has been removed by an extensive wash (right bar). The anisotropy was determined as described in the Experimental Procedures.

wavelength of 480 nm was used (Figure 5A). Decreasing the polarity of the solvent surrounding the fluorophore by addition of increasing concentrations of dioxane caused a dramatic elevation in the fluorescence quantum yield and an associated blue-shift of the emission λ_{MAX} (Figure 5A). Using this biophysical property of IANBD, inferences about the molecular environment of putative IANBD labeling site-(s) might be possible. As shown in Figure 5B, the IANBD labeled hSERT has a λ_{MAX} of 528 nm corresponding to the fluorescence from free IANBD in dioxane/water mixtures (v/v) containing more than 95% dioxane. This would suggest that IANBD is labeling cysteine(s) embedded in highly hydrophobic environments. Note that, as a consequence hereof, labeling of cysteines exposed to the aqueous environment cannot be inferred as the emission from these likely are minor as compared to the fluorescence from the hydrophobic sites.

Evidence for ^{109}Cys as a Major IANBD Fluorescence Site. Next we investigated the accessibility of IANBD covalently attached to the transporter in collisional quenching experiments. Collisional quenching requires a bimolecular interaction between the quencher and the fluorophore, and, therefore, such experiments can determine directly the accessibility of the fluorophore to the surrounding environment. The aqueous quencher iodide (I^-) was able to cause a marked quenching of the fluorescence of the IANBD labeled transporter. This is illustrated by the linear Stern−Volmer plot in Figure 6A in which F_0/F is plotted against the potassium iodide concentration. The slope of the line represents the Stern−Volmer constant (K_{sv}), which was 3.4 $\pm$ 0.10 M^{-1} for the IANBD labeled hSERT. The fluorescence quenching by iodide was considerably reduced in the labeled hSERT mutant 5CysKO where five cysteines were knocked out, displaying a K_{sv} value of 2.1 $\pm$ 0.16 M^{-1} (Figure 6B). The single cysteine knock-out mutant (C109A, Figure 6C) is entirely responsible for the quenching phenotype seen in the 5CysKO mutant (Figure 6B) as it was quenched with a K_{sv} of 2.2 $\pm$ 0.15 M^{-1}. These data strongly suggest ^{109}Cys as a labeling site that contributes considerably to the overall fluorescence of the IANBD labeled SERT. Due to the environmentally sensitive nature of the NBD fluorophore,

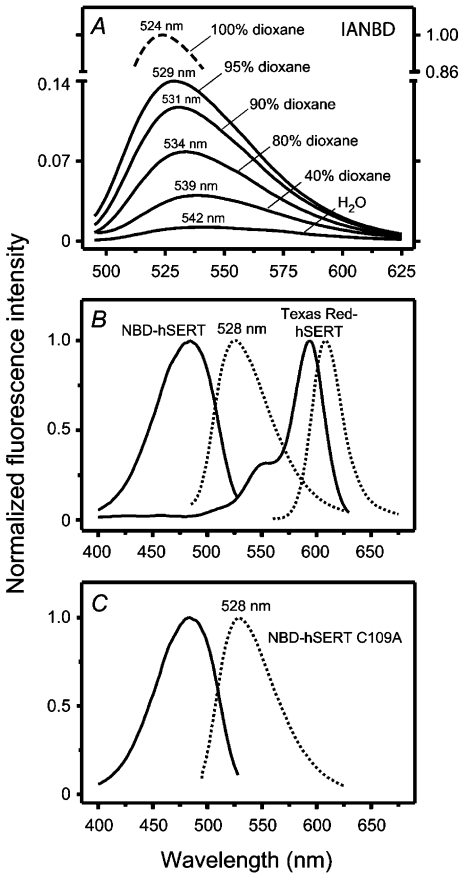

FIGURE 5: Fluorescent properties of IANBD free in solution and of IANBD and Texas Red labeled hSERT. (A) Emission spectra of free IANBD in dioxane/water. The fraction of dioxane ranges from 0% to 100% (v/v) in selected intervals. (B) Excitation (solid line) and emission (dashed line) spectra of the purified and IANBD or Texas Red labeled hSERT. The emission maximum (λ_{MAX}) of the IANBD labeled transporter (NBD-hSERT) is 528 nm as indicated. (C) Excitation (solid line) and emission (dashed line) spectra of the purified and IANBD labeled hSERT-C109A with an emission λ_{MAX} of 528 nm. The spectra shown are representative of three independent purification and fluorophore labeling experiments.

the data also suggest that ^{109}Cys is embedded in a hydrophobic environment that nevertheless is in close contact with the aqueous phase.

Besides ^{109}Cys, one or more additional hydrophobic labeling sites exist in the transporter since replacing ^{109}Cys with alanine does not change the λ_{MAX} of IANBD labeled hSERT-C109A (Figure 5C, dashed line spectra) compared to IANBD labeled hSERT (Figure 5B, dashed line spectra). These observations are supported by experiments using the lipid-soluble short-range quencher of fluorescence 2,2,6,6-tetramethylpiperidine-*N*-oxyl (TEMPO). TEMPO quenching experiments on IANBD labeled hSERT and hSERT-C109A resulted in Stern−Volmer quenching constants (K_{sv}) of 72.4 $\pm$ 1.9 (n = 3) and 71.3 $\pm$ 1.7 (n = 3), respectively (Figure 7). The removal of ^{109}Cys does not change the TEMPO quenching, suggesting that ^{109}Cys is equally sensitive for TEMPO quenching as the remaining hydrophobic labeling site(s) combined.

Effect of Substrate, Inhibitors, and Ions on Fluorescence from IANBD or Texas Red Labeled SERT. The possibility of assessing time-resolved ligand induced conformational changes of the purified and fluorescently labeled SERT was

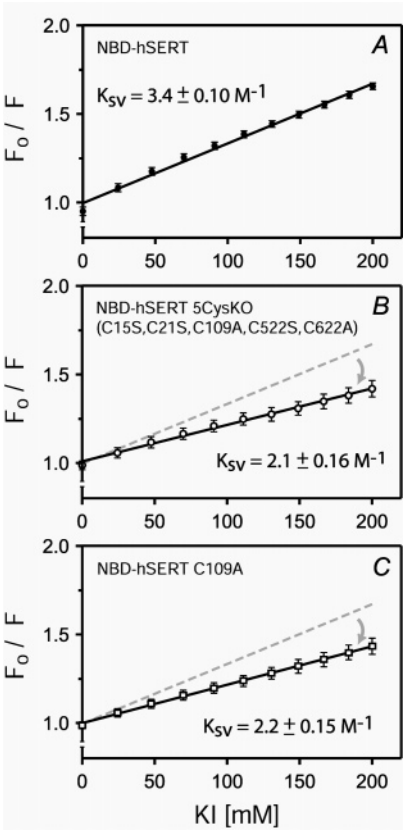

FIGURE 6: Fluorescence quenching of the IANBD labeled transporter by potassium iodide. Stern−Volmer plots showing collisional quenching of NBD fluorescence by the water-soluble quencher potassium iodide (KI). (A) IANBD labeled hSERT (NBD-hSERT). (B) IANBD labeled hSERT-5CysKO (NBD-hSERT 5CysKO). (C) IANBD labeled hSERT-C109A (NBD-hSERT C109A). The broken shaded lines in panels B and C represent the IANBD labeled hSERT in *A*. The quenching experiments were carried out, and the data was plotted as described in the Experimental Procedures. The Stern−Volmer quenching constants (K_{sv}) were 3.4 ± 0.10 M^{-1}, 2.1 ± 1.6 M^{-1}, and 2.2 ± 1.5 M^{-1} (means ± SE, n = 3) for the IANBD labeled hSERT, hSERT-5CysKO, and hSERT-C109A, respectively. In all experiments the excitation was 480 nm and the emission was recorded at 528 nm.

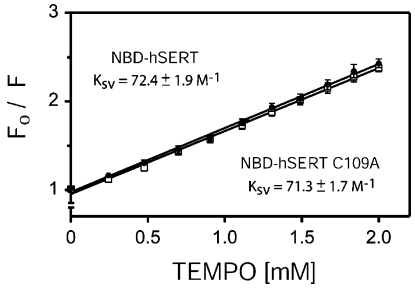

FIGURE 7: Fluorescence quenching of the IANBD labeled transporter by TEMPO. Stern−Volmer plots showing collisional quenching of NBD fluorescence by the lipid-soluble quencher TEMPO. Filled circles: IANBD labeled hSERT (NBD-hSERT). Open squares: IANBD labeled hSERT-C109A (NBD-hSERT C109A). The quenching experiments were carried out, and the data was plotted as described in the Experimental Procedures. The Stern−Volmer quenching constants (K_{sv}) were 72.4 ± 1.9 M^{-1} and 71.3 ± 1.7 M^{-1} (means ± SE, n = 3) for the IANBD labeled hSERT and hSERT-C109A, respectively. In all experiments the excitation was 480 nm and the emission was recorded at 528 nm.

a major objective of this study. Accordingly, hSERT labeled with IANBD or Texas Red (15−25 pmol in buffer containing 0.05% digitonin) were subject to a spectroscopic analysis in which fluorescence emission at a fixed optimal wavelength was measured over time at a fixed optimal excitation wavelength. Following achievement of a stable baseline fluorescence under magnetic stirring, the effect of adding 5-HT (1−10 μM_{final}), RTI-55 (1−10 μM_{final}), citalopram (1−10 μM_{final}), NaCl or LiCl (100 mM_{final} in NaCl free buffer) was recorded for at least 500 s. However, we were unable to detect any reproducible changes from the baseline in response to any of these compounds. We also tried several other sulfhydryl-reactive fluorescent probes including anilinonaphthalene-sulfonate, monobromobimane, fluorescein maleimide, and coumarin maleimide with a similar negative result (data not shown).

DISCUSSION

In this study we have developed the critical methods for performing direct structural studies on the human serotonin transporter (hSERT). The transporter was expressed in Sf9 insect cells, and a purification procedure was established. This procedure allowed purification of transporter in larger amount and of higher purity than described previously; hence, although purification of the SERT has been described several times before, it has only been purified from native tissues in total yields of less than 10 pmol with a generally low purity (*27*, *37*−*40*). Of the Na^+/Cl^- coupled transporters, successful purification has only been reported before for the GABA transporter-1 (*41*, *42*). Using the present procedure we were able to purify ∼0.1 mg of hSERT per liter of insect cell culture. This is sufficient for performing biophysical studies based on e.g. fluorescent labeling (see below). Importantly, we were able at least in part to circumvent the inherent problem of the Sf9 insect cell system that a large fraction of the expressed protein does not undergo proper folding and maturation (*25*, *34*, *43*). First, we expressed the protein in the presence of the molecular chaperone calnexin (*25*), and second we purified selectively glycosylated and thus mature protein by using concanavalin A chromatography. In this way, we were able to obtain purified transport protein of which around 80% was active as assessed by the ability of the protein to bind radiolabeled RTI-55.

The pharmacological properties of the purified protein were similar to those observed in native tissue, suggesting that the overall tertiary structure of the transporter has been conserved after purification and thus that it was in an active conformation. The affinity of 5-HT was 10-fold higher in the purified preparation as compared to that observed in the corresponding membranes. Similarly, the affinity for imipramine increased from 13.5 nM to 1.5 nM (Table 2). One conceivable explanation would be that the detergent (digitonin) constrains the transporter in a conformation that is more favorable for binding these compounds. Interestingly, increased affinity for agonists was previously reported for the β2 adrenergic receptor upon solublization in digitonin consistent with the ability of digitonin to constrain the receptor in a high-affinity state for agonists (*44*). It should also be taken into account that the phenomenon of substrate affinity changes for SERT as compared to native tissue has been seen before in other overexpression studies (*45*, *46*). It could accordingly be considered that an "endogenous factor", such as critical lipid or associated proteins, that affects the affinity of substrate binding to SERT exists. Such a factor still needs to be identified; however, it is important to point

out that the affinity change seen upon purification may reflect the absence or presence of a SERT modulator rather than a fundamental alteration of SERT tertiary structure.

We have not yet been able to assess whether the purified transporter, although capable of binding substrates and inhibitor, is fully functional and thus able to transport. To address this question, functional reconstitution of the purified protein into liposomes is required, but we have so far not been able to accomplish this. The SERT has previously been functionally reconstituted into liposomes from platelets or placental brush border cells extracted in cholate or digitonin (*39*, *47*, *48*). In parallel to the considerations in the previous paragraph, it is interesting to consider the possibility that our purification procedure removes essential lipids or associated proteins critical for achieving functional reconstitution. Another problem is the sensitivity of the purified transporter to different detergents. Out of 40 different tested detergents (DSOL-90-10 solution master detergent kit from Anatrace Inc., Maumee, OH) the purified transporter only preserved its ability to bind radiolabeled RTI-55 in digitonin (data not shown). Unfortunately, this detergent is particularly difficult to remove during reconstitution due to its very low critical micelle concentration (CMC).

A major purpose of establishing an efficient purification procedure was to implement the use of spectroscopic techniques in our study of the monoamine transporters. Previously, we have successfully used fluorescence spectroscopy to characterize ligand-induced conformational changes in the purified β_2 adrenergic receptor. In particular, we took advantage of fluorescent molecules with an emission displaying high sensitivity to the polarity of the surrounding environment such as NBD (nitrobenxoxadiazol). On the basis of the spectroscopic analyses it was possible, for example, to deduce a key role of TM 6 movements for agonist activation of the receptor (*16*−*18*). The use of fluorescent techniques has also previously been successfully applied to other transport proteins such as the Lac permease from *E. coli* (*20*, *21*, *49*, *50*).

To implement the use of fluorescent techniques, we analyzed first the consequences of labeling the purified hSERT with either IANBD or another sulfhydryl reactive fluorophore, Texas Red bromoacetamide. This labeling was compared to that seen in Sf9 cell membranes. Overall, labeling was well-tolerated by the transporter. Using 100−200 μM fluorophore we could derivatize endogenous cysteines in the purified transporter without any major interference with ligand binding (Tables 2 and 3). Specifically, we observed no effect on the B_{MAX} for [^{125}I]RTI-55 binding in response to IANBD or Texas Red bromoacetamide either in membranes or on the purified transporter; however, labeling was accompanied by a small decrease in affinity for [^{125}I]RTI-55 (Table 4). A similar decrease in affinity was observed upon MTSEA labeling (Table 4). This decrease is likely to explain previous reports showing a marked decrease in response to MTSEA in binding when using a subsaturating concentration of [^{125}I]RTI-55 (B_0) (Figure 3) (*35*). Interestingly, the decrease in affinity in response to IANBD and Texas Red bromoacetamide was eliminated upon mutation of ^{109}Cys, suggesting that the decrease in affinity was caused by labeling of this cysteine and thus that derivatization of ^{109}Cys with fluorescent labels has a minor structural impact on the transporter (Table 3 and data not shown). The effect of MTSEA was nonetheless not eliminated in either 5CysKO or C109A (data not shown). This agrees with previous observations suggesting that the inhibitory effect of MTSEA on [^{125}I]RTI-55 binding is the result of labeling not only ^{109}Cys but also ^{357}Cys (*35*).

The data raise the question whether IANDB/ Texas Red bromoacetamide label a different subset of cysteines than MTSEA, or, alternatively, they label the same subset of cysteines but labeling with a hydrophobic fluorophore has a different impact on transporter structure and transporter function than labeling with the positively charged MTSEA group. Since IANBD was unable to protect against the effect of MTSEA in an experiment where we labeled with IANBD prior to MTSEA and compared to MTSEA alone (data not shown), it is most likely that IANBD and MTSEA display different labeling patterns. This is also not surprising given the different chemistry by which the cysteines are labeled (MTS versus iodacetamide and bromoacetamide), which might profoundly affect the reactivity of the individual cysteines. The reaction between sulfhydryls and MTS reagents occurs, for example, a billion times faster in an aqueous solution; hence, MTS reagents are in contrast to iodoacetamide reagents unlikely to label cysteines buried in a hydrophobic nonaqueous environment and, therefore, a completely different labeling pattern could be obtained with the different sulfhydryl-reactive compounds.

The hSERT contains 18 cysteines of which two in the second extracellular loop are believed to form a disulfide bridge (*51*, *52*) leaving 16 cysteines potentially available for chemical derivatization. Because the estimated stoichiometry of the labeling was ∼4−5 mol/mol of WT transporter (data not shown), we were labeling at least four and probably several more of these cysteines since some sites likely are not completely labeled. Upon mutating the five cysteines in 5CysKO the estimated stoichiometry of labeling was reduced about one-third from WT labeling for both fluorophores (data not shown). For C109A the estimated stoichiometry of labeling was reduced about one-sixth of WT labeling for both fluorophores (data not shown). Thus, even upon removal of 5 cysteines outside the transmembrane regions we had considerable labeling consistent with labeling of sites in these parts of the transporter. In light of the dependency of IANDB emission on the molecular environment, the labeling of transmembrane cysteines was also supported by the spectroscopic analyses showing a λ_{MAX} of the emission from the labeled transporter, which corresponds to that observed in 95−100% dioxane, and by the observation that the hydrophobic short range quencher of fluorescence, TEMPO, strongly quenched the IANBD fluorescence (Figure 7). In this context it is important to emphasize that, due to the environmentally sensitive nature of IANBD, the fluorescence emission from sites in a hydrophobic milieu will strongly dominate other labeling sites exposed to more polar environments. Thus, there is no direct correlation between the degree of labeling of a given site and the contribution to the overall fluorescence.

The present data suggest that one of the IANBD labeling sites is ^{109}Cys. Mutation of this residue reduced substantially the quenching by the water soluble quencher iodide. This suggests first of all that ^{109}Cys is being labeled and that the fluorescence from this site contributes significantly to the overall fluorescence from the labeled transporter (Figure 6).

We were unable to see a difference in the absolute fluorescence when comparing labeled wild type with C109A most likely because the total fluorescence is a highly sensitive and poor quantitative measure that inevitably varies between different labelings/purifications. Most importantly, the ability of iodide to quench the ^{109}Cys fluorescence also suggested that this residue must be located in a mixed hydrophobic/hydrophilic environment. The ability of iodide to quench the fluorescence requires at least partial exposure to the aqueous milieu whereas its contribution to the overall fluorescence requires a hydrophobic microenvironment. Such a milieu is only found at the membrane/micelle boundary, and thus the data support a partially buried location of ^{109}Cys in the short extracellular loop connecting TM1 and 2. In addition, the findings for ^{109}Cys correspond well to our previous observation for a stretch of cysteines inserted at membrane/micelle boundary at the intracellular end of TM 6 in the β_2 adrenergic receptor (*18*). It is also of interest that the quenching in response to TEMPO did not change upon mutation of ^{109}Cys (Figure 7). This indicates that TEMPO is quenching the fluorescence from other sites that are more protected from aqueous iodide than of ^{109}Cys and thus buried deeper in the transporter structure.

Our current insight into ligand and solute induced conformational changes in the monoamine transporters is mainly based on studies involving indirect measures such as probing the effect on substrate translocation and/or inhibitor binding following labeling of endogenous or engineered cysteines with MTS-compounds (*53*−*58*) and the engineering of metal ion binding sites (*3*, *4*, *59*). However, labeling of the SERT and the GABA transporter-1 with conformationally sensitive fluorophores directly in oocytes has recently been carried out (*60*, *61*). The power of this technique is the possibility of assessing fluorescence changes and performing electrophysiological recordings simultaneously. The major drawback is the unavoidable background due to labeling of irrelevant proteins. One consequence of this is, for example, that the technique only allows detection of putative conformational changes in extracellularly facing transporter structures because it is only possible to use membrane impermeable thiol- or amine-reactive fluorescent probes to prevent labeling of irrelevant intracellular proteins. To enable the study of conformational changes deep within the transmembrane domain and at sites exposed to the intracellular side in a time-resolved manner, it is therefore necessary to use a purified preparation of the transporter. We were, nonetheless, unable to observe any changes in fluorescence from the IANBD or Texas Red labeled purified hSERT in response to either substrates or inhibitors or ions. This indicates that the labeled cysteines either do not move upon substrate/inhibitor/ion binding or, more likely, that they move but not in a way that significantly alters the polarity of the environment surrounding the attached fluorophore. The absence of measurable fluorescent changes might also be a consequence of labeling several cysteines that could mask an emission change at a single site. Our inability to detect conformational changes using fluorescent techniques is not due to the fact that our purified preparation of the SERT cannot undergo conformational changes. We have by application of a chemical cleavage approach (*62*, *63*) obtained evidence for distinct structural changes in the transporter molecule in response to 5-HT, cocaine analogues, and selective serotonin reuptake inhibitors (SSRIs) (Rasmussen and Gether, unpublished observation). Thus, the future strategy will be to insert new cysteines into positions predicted to be in conformationally active domains. Another important prospect of having an efficient purification procedure of a monoamine transporter is the possibility of studying the structural basis and functional consequences of protein−protein interactions with known regulatory proteins such as PP2A (*64*) and syntaxin 1A (*65*) in an isolated reconstituted system.

ACKNOWLEDGMENT

We thank Dr. Ivy Carrol for providing unlabeled RTI-55, Dr. Chris Tate for the baculovirus encoding calnexin, and Dr. Randy Blakely for the cDNA encoding the hSERT. We thank Lis Sørensen for technical assistance and Drs. Jonathan Javitch and Claus Juul Løland for critical reading of the manuscript.

REFERENCES

1. Norregaard, L., and Gether, U. (2001) The monoamine neurotransmitter transporters: structure, conformational changes and molecular gating, *Curr. Opin. Drug Discov. Dev. 4*, 591−601.
2. Chen, N., and Reith, M. E. (2000) Structure and function of the dopamine transporter, *Eur. J. Pharmacol. 405*, 329−339.
3. Norregaard, L., Frederiksen, D., Nielsen, E. O., and Gether, U. (1998) Delineation of an endogenous zinc-binding site in the human dopamine transporter, *EMBO J. 17*, 4266−4273.
4. Loland, C. J., Norregaard, L., and Gether, U. (1999) Defining proximity relationships in the tertiary structure of the dopamine transporter. Identification of a conserved glutamic acid as a third coordinate in the endogenous Zn(2+)-binding site, *J. Biol. Chem. 274*, 36928−36934.
5. Norregaard, L., Visiers, I., Loland, C. J., Ballesteros, J., Weinstein, H., and Gether, U. (2000) Structural Probing of a Microdomain in the Dopamine Transporter by Engineering of Artificial Zn(2+) Binding Sites, *Biochemistry 39*, 15836−15846.
6. MacAulay, N., Bendahan, A., Loland, C. J., Zeuthen, T., Kanner, B. I., and Gether, U. (2001) Engineered Zn(2+) switches in the GABA transporter-1: differential effects on GABA uptake and currents, *J. Biol. Chem. 276*, 40476−40485.
7. Mitchell, S. M., Lee, E., Garcia, M. L., and Stephan, M. M. (2004) Structure and function of extracellular loop 4 of the serotonin transporter as revealed by cysteine-scanning mutagenesis, *J. Biol. Chem. 279*, 24089−24099.
8. Ju, P., Aubrey, K. R., and Vandenberg, R. J. (2004) Zn2+ inhibits glycine transport by glycine transporter subtype 1b, *J. Biol. Chem. 279*, 22983−22991.
9. Hastrup, H., Karlin, A., and Javitch, J. A. (2001) Symmetrical dimer of the human dopamine transporter revealed by cross-linking Cys-306 at the extracellular end of the sixth transmembrane segment, *Proc. Natl. Acad. Sci. U.S.A. 98*, 10055−10060.
10. Kilic, F., and Rudnick, G. (2000) Oligomerization of serotonin transporter and its functional consequences, *Proc. Natl. Acad. Sci. U.S.A. 97*, 3106−3111.
11. Schmid, J. A., Scholze, P., Kudlacek, O., Freissmuth, M., Singer, E. A., and Sitte, H. H. (2000) Oligomerization of the human serotonin transporter and of the rat GABA transporter 1 visualized by fluorescence resonance energy transfer microscopy in living cells, *J. Biol. Chem. 276*, 3805−3810.
12. Norgaard-Nielsen, K., Norregaard, L., Hastrup, H., Javitch, J. A., and Gether, U. (2002) Zn(2+) site engineering at the oligomeric interface of the dopamine transporter, *FEBS Lett. 524*, 87−91.
13. Abramson, J., Smirnova, I., Kasho, V., Verner, G., Kaback, H. R., and Iwata, S. (2003) Structure and mechanism of the lactose permease of Escherichia coli, *Science 301*, 610−615.
14. Huang, Y., Lemieux, M. J., Song, J., Auer, M., and Wang, D. N. (2003) Structure and mechanism of the glycerol-3-phosphate transporter from Escherichia coli, *Science 301*, 616−620.
15. Torres, G. E., Gainetdinov, R. R., and Caron, M. G. (2003) Plasma membrane monoamine transporters: structure, regulation and function, *Nat. Rev. Neurosci. 4*, 13−25.

16. Gether, U., Lin, S., Ghanouni, P., Ballesteros, J. A., Weinstein, H., and Kobilka, B. K. (1997) Agonists induce conformational changes in transmembrane domains III and VI of the beta2 adrenoceptor, *EMBO J. 16*, 6737−6747.
17. Gether, U., Lin, S., and Kobilka, B. K. (1995) Fluorescent labeling of purified beta2-adrenergic receptor: Evidence for ligand-specific conformational changes, *J. Biol. Chem. 270*, 28268−28275.
18. Jensen, A. D., Guarnieri, F., Rasmussen, S. G., Asmar, F., Ballesteros, J. A., and Gether, U. (2001) Agonist-induced conformational changes at the cytoplasmic side of TM 6 in the beta2-adrenergic receptor mapped by site-selective fluorescent labeling, *J. Biol. Chem. 276*, 9279−9290.
19. Ghanouni, P., Steenhuis, J. J., Farrens, D. L., and Kobilka, B. K. (2001) Agonist-induced conformational changes in the G-protein-coupling domain of the beta2-adrenergic receptor, *Proc. Natl. Acad. Sci. U.S.A. 98*, 5997−6002.
20. Wang, Q., Matsushita, K., de Foresta, B., le Maire, M., and Kaback, H. R. (1997) Ligand-induced movement of helix X in the lactose permease from Escherichia coli: a fluorescence quenching study, *Biochemistry 36*, 14120−14127.
21. Jung, K., Jung, H., and Kaback, H. R. (1994) Dynamics of lactose permease of Escherichia coli determined by site-directed fluorescence labeling, *Biochemistry 33*, 3980−3985.
22. Rosenqvist, N., Hard Af Segerstad, C., Samuelsson, C., Johansen, J., and Lundberg, C. (2002) Activation of silenced transgene expression in neural precursor cell lines by inhibitors of histone deacetylation, *J. Gene Med. 4*, 248−257.
23. Lakovicz, J. R. (1999) *Principles of fluorescence spectroscopy*, 2nd ed., Kluwer Academic/Plenum Publishers, New York.
24. London, E. (1986) A fluorescence-based detergent binding assay for protein hydrophobicity, *Anal. Biochem. 154*, 57−63.
25. Tate, C. G., Whiteley, E., and Betenbaugh, M. J. (1999) Molecular chaperones stimulate the functional expression of the cocaine-sensitive serotonin transporter, *J. Biol. Chem. 274*, 17551−17558.
26. Boja, J. W., Mitchell, W. M., Patel, A., Kopajtic, T. A., Carroll, F. I., Lewin, A. H., Abraham, P., and Kuhar, M. J. (1992) High-affinity binding of [125I]RTI-55 to dopamine and serotonin transporters in rat brain, *Synapse 12*, 27−36.
27. Launay, J. M., Geoffroy, C., Mutel, V., Buckle, M., Cesura, A., Alouf, J. E., and Da Prada, M. (1992) One-step purification of the serotonin transporter located at the human platelet plasma membrane, *J. Biol. Chem. 267*, 11344−11351.
28. Rothman, R. B., Cadet, J. L., Akunne, H. C., Silverthorn, M. L., Baumann, M. H., Carroll, F. I., Rice, K. C., de Costa, B. R., Partilla, J. S., Wang, J. B., et al. (1994) Studies of the biogenic amine transporters. IV. Demonstration of a multiplicity of binding sites in rat caudate membranes for the cocaine analog [125I]RTI-55, *J. Pharmacol. Exp. Ther. 270*, 296−309.
29. Adkins, E. M., Barker, E. L., and Blakely, R. D. (2001) Interactions of Tryptamine Derivatives with Serotonin Transporter Species Variants Implicate Transmembrane Domain I in Substrate Recognition, *Mol. Pharmacol. 59*, 514−523.
30. Barker, E. L., Moore, K. R., Rakhshan, F., and Blakely, R. D. (1999) Transmembrane domain I contributes to the permeation pathway for serotonin and ions in the serotonin transporter, *J. Neurosci. 19*, 4705−4717.
31. Barker, E. L., Perlman, M. A., Adkins, E. M., Houlihan, W. J., Pristupa, Z. B., Niznik, H. B., and Blakely, R. D. (1998) High affinity recognition of serotonin transporter antagonists defined by species-scanning mutagenesis. An aromatic residue in transmembrane domain I dictates species-selective recognition of citalopram and mazindol, *J. Biol. Chem. 273*, 19459−19468.
32. Eshleman, A. J., Carmolli, M., Cumbay, M., Martens, C. R., Neve, K. A., and Janowsky, A. (1999) Characteristics of drug interactions with recombinant biogenic amine transporters expressed in the same cell type, *J. Pharmacol. Exp. Ther. 289*, 877−885.
33. Ramamoorthy, S., Bauman, A. L., Moore, K. R., Han, H., Yang-Feng, T., Chang, A. S., Ganapathy, V., and Blakely, R. D. (1993) Antidepressant- and cocaine-sensitive human serotonin transporter: molecular cloning, expression, and chromosomal localization, *Proc. Natl. Acad. Sci. U.S.A. 90*, 2542−2546.
34. Tate, C. G., and Blakely, R. D. (1994) The effect of N-linked glycosylation on activity of the Na(+)- and Cl(−)-dependent serotonin transporter expressed using recombinant baculovirus in insect cells, *J. Biol. Chem. 269*, 26303−26310.
35. Androutsellis-Theotokis, A., Ghassemi, F., and Rudnick, G. (2001) A conformationally sensitive residue on the cytoplasmic surface of serotonin transporter, *J. Biol. Chem. 276*, 45933−45938.
36. Rasmussen, S. G., Carroll, F. I., Maresch, M. J., Jensen, A. D., Tate, C. G., and Gether, U. (2001) Biophysical characterization of the cocaine binding pocket in the serotonin transporter using a fluorescent cocaine analogue as a molecular reporter, *J. Biol. Chem. 276*, 4717−4723.
37. Biessen, E. A., Horn, A. S., and Robillard, G. T. (1990) Partial purification of the 5-hydroxytryptamine-reuptake system from human blood platelets using a citalopram-derived affinity resin, *Biochemistry 29*, 3349−3354.
38. Graham, D., Esnaud, H., and Langer, S. Z. (1992) Partial purification and characterization of the sodium-ion-coupled 5-hydroxytryptamine transporter of rat cerebral cortex, *Biochem. J. 286*, 801−805.
39. Ramamoorthy, S., Leibach, F. H., Mahesh, V. B., and Ganapathy, V. (1993) Partial purification and characterization of the human placental serotonin transporter, *Placenta 14*, 449−461.
40. Rotondo, A., Giannaccini, G., Betti, L., Chiellini, G., Marazziti, D., Martin, C., Lucacchini, A., and Cassano, G. B. (1996) The serotonin transporter from human brain: purification and partial characterization, *Neurochem. Int. 28*, 299−307.
41. Radian, R., and Kanner, B. I. (1985) Reconstitution and purification of the sodium- and chloride-coupled gamma-aminobutyric acid transporter from rat brain, *J. Biol. Chem. 260*, 11859−11865.
42. Radian, R., Bendahan, A., and Kanner, B. I. (1986) Purification and identification of the functional sodium- and chloride-coupled gamma-aminobutyric acid transport glycoprotein from rat brain, *J. Biol. Chem. 261*, 15437−15441.
43. Melikian, H. E., McDonald, J. K., Gu, H., Rudnick, G., Moore, K. R., and Blakely, R. D. (1994) Human norepinephrine transporter. Biosynthetic studies using a site-directed polyclonal antibody, *J. Biol. Chem. 269*, 12290−12297.
44. Samama, P., Cotecchia, S., Costa, T., and Lefkowitz, R. J. (1993) A mutation-induced activated state of the beta2-adrenergic receptor: Extending the ternary complex model, *J. Biol. Chem. 268*, 4625−4636.
45. Ramsey, I. S., and DeFelice, L. J. (2002) Serotonin transporter function and pharmacology are sensitive to expression level: evidence for an endogenous regulatory factor, *J. Biol. Chem. 277*, 14475−14482.
46. Tate, C. G., Haase, J., Baker, C., Boorsma, M., Magnani, F., Vallis, Y., and Williams, D. C. (2003) Comparison of seven different heterologous protein expression systems for the production of the serotonin transporter, *Biochim. Biophys. Acta 1610*, 141−153.
47. Rudnick, G., and Nelson, P. J. (1978) Reconstitution of 5-hydroxytryptamine transport from cholate-disrupted platelet plasma membrane vesicles, *Biochemistry 17*, 5300−5303.
48. Ramamoorthy, S., Cool, D. R., Leibach, F. H., Mahesh, V. B., and Ganapathy, V. (1992) Reconstitution of the human placental 5-hydroxytryptamine transporter in a catalytically active form after detergent solubilization, *Biochem. J. 286*, 89−95.
49. Smirnova, I. N., and Kaback, H. R. (2003) A mutation in the lactose permease of Escherichia coli that decreases conformational flexibility and increases protein stability, *Biochemistry 42*, 3025−3031.
50. Vazquez-Ibar, J. L., Weinglass, A. B., and Kaback, H. R. (2002) Engineering a terbium-binding site into an integral membrane protein for luminescence energy transfer, *Proc. Natl. Acad. Sci. U.S.A. 99*, 3487−3492.
51. Wang, J. B., Moriwaki, A., and Uhl, G. R. (1995) Dopamine transporter cysteine mutants: second extracellular loop cysteines are required for transporter expression, *J. Neurochem. 64*, 1416−1419.
52. Sur, C., Schloss, P., and Betz, H. (1997) The rat serotonin transporter: identification of cysteine residues important for substrate transport, *Biochem. Biophys. Res. Commun. 241*, 68−72.
53. Chen, J. G., Sachpatzidis, A., and Rudnick, G. (1997) The third transmembrane domain of the serotonin transporter contains residues associated with substrate and cocaine binding, *J. Biol. Chem. 272*, 28321−28327.
54. Ferrer, J., and Javitch, J. A. (1998) Cocaine alters the accessibility of endogenous cysteines in putative extracellular and extracellular loops of the human dopamine transporter, *Proc. Natl. Acad. Sci. U.S.A. 95*, 9238−9243.
55. Chen, J. G., and Rudnick, G. (2000) Permeation and gating residues in serotonin transporter, *Proc. Natl. Acad. Sci. U.S.A. 97*, 1044−1049.

56. Chen, N., Ferrer, J. V., Javitch, J. A., and Justice, J. B., Jr. (2000) Transport-dependent accessibility of a cytoplasmic loop cysteine in the human dopamine transporter, *J. Biol. Chem. 275*, 1608−1614.
57. Sato, Y., Zhang, Y. W., Androutsellis-Theotokis, A., and Rudnick, G. (2004) Analysis of transmembrane domain 2 of rat serotonin transporter by cysteine scanning mutagenesis, *J. Biol. Chem. 279*, 22926−22933.
58. Norregaard, L., Loland, C. J., and Gether, U. (2003) Evidence for distinct sodium-, dopamine-, and cocaine-dependent conformational changes in transmembrane segments 7 and 8 of the dopamine transporter, *J. Biol. Chem. 278*, 30587−30596.
59. Loland, C. J., Norregaard, L., Litman, T., and Gether, U. (2002) Generation of an activating Zn(2+) switch in the dopamine transporter: mutation of an intracellular tyrosine constitutively alters the conformational equilibrium of the transport cycle, *Proc. Natl. Acad. Sci. U.S.A. 99*, 1683−1688.
60. Li, M., and Lester, H. A. (2002) Early fluorescence signals detect transitions at mammalian serotonin transporters, *Biophys. J. 83*, 206−218.
61. Li, M., Farley, R. A., and Lester, H. A. (2000) An intermediate state of the gamma-aminobutyric acid transporter GAT1 revealed by simultaneous voltage clamp and fluorescence, *J. Gen. Physiol. 115*, 491−508.
62. Goldshleger, R., and Karlish, S. J. (1997) Fe-catalyzed cleavage of the alpha subunit of Na/K-ATPase: evidence for conformation-sensitive interactions between cytoplasmic domains, *Proc. Natl. Acad. Sci. U.S.A. 94*, 9596−9601.
63. Wu, J., Perrin, D. M., Sigman, D. S., and Kaback, H. R. (1995) Helix packing of lactose permease in Escherichia coli studied by site-directed chemical cleavage, *Proc. Natl. Acad. Sci. U.S.A. 92*, 9186−9190.
64. Bauman, A. L., Apparsundaram, S., Ramamoorthy, S., Wadzinski, B. E., Vaughan, R. A., and Blakely, R. D. (2000) Cocaine and antidepressant-sensitive biogenic amine transporters exist in regulated complexes with protein phosphatase 2A, *J. Neurosci. 20*, 7571−7578.
65. Quick, M. W. (2003) Regulating the conducting states of a mammalian serotonin transporter, *Neuron 40*, 537−549.

BI048022B